View metadata, citation and similar papers at core.ac.uk

brought to you by CORE

provided by DSpace@MIT

NIH Public Access
Author Manuscript
Oncogene. Author manuscript; available in PMC 2014 July 14.

Published in final edited form as:
Oncogene. 2014 July 10; 33(28): 3742–3747. doi:10.1038/onc.2013.333.

Bmi1 is required for tumorigenesis in a mouse model of intestinal cancer

Mindy A. Maynard[1], **Roberta Ferretti**[1], **Keren I. Hilgendorf**[1,2], **Christine Perret**[3], **Peter Whyte**[4], and **Jacqueline A. Lees**[1,2]

[1]Koch Institute for Integrative Cancer Research at Massachusetts Institute of Technology, Cambridge MA 02139, USA

[2]Department of Biology, Massachusetts Institute of Technology, Cambridge MA 02139, USA

[3]Institut Cochin-INSERM, Universite Paris V, 75014 Paris, France

[4]Department of Pathology and Molecular Medicine, McMaster University, Hamilton ON L8S 4L8, Canada

Abstract

The epigenetic regulator BMI1 is upregulated progressively in a wide variety of human tumors including colorectal cancer. In this study, we assessed the requirement for *Bmi1* in intestinal tumorigenesis using an autochthonous mouse model in which *Apc* was conditionally ablated in the intestinal epithelium. Germline mutation of *Bmi1* significantly reduced both the number and size of small intestinal adenomas arising in this model, and it acted in a dose-dependent manner. Moreover, in contrast to wildtype controls, *Bmi1*$^{-/-}$ mice showed no increase in median tumor size, and a dramatic decrease in tumor number, between 3 and 4 months of age. Thus, *Bmi1* is required for both progression and maintenance of small intestinal adenomas. Importantly, Bmi1 deficiency did not disrupt oncogenic events arising from *Apc* inactivation. Instead, the *Arf* tumor suppressor, a known target of Bmi1 epigenetic silencing, was upregulated in *Bmi1* mutant tumors. This was accompanied by significant upregulation of p53, which was confirmed by sequencing to be wildtype, and also elevated apoptosis within the smallest Bmi1$^{-/-}$ adenomas. By crossing *Arf* into this cancer model, we showed that *Arf* is required for the induction of both p53 and apoptosis, and it is a key determinant of the ability of *Bmi1* deficiency to suppress intestinal tumorigenesis. Finally, a conditional *Bmi1* mutant strain was generated and used to determine the consequences of deleting *Bmi1* specifically within the intestinal epithelium. Strikingly, intestinal-specific *Bmi1* deletion suppressed small intestinal adenomas in a manner that was indistinguishable from germline *Bmi1* deletion. Thus, we conclude that *Bmi1* deficiency impairs the progression and maintenance of small intestinal tumors in a cell autonomous and highly *Arf*-dependent manner.

Keywords

Bmi1; Apc; colorectal cancer; intestine; apoptosis; Arf

Correspondence to: Jacqueline A. Lees.

Conflict of Interests There are no competing financial interests in relation to the work described.

NIH-PA Author Manuscript

NIH-PA Author Manuscript

NIH-PA Author Manuscript

NIH-PA Author Manuscript
NIH-PA Author Manuscript
NIH-PA Author Manuscript

Introduction

Colorectal carcinoma (CRC) is the 4th leading cause of cancer deaths worldwide, resulting in over 600,000 fatalities a year (1). Upregulation of Wnt pathway activity, through loss of the *Apc* tumor suppressor or deregulation of the β-catenin proto-oncogene, is an early event in the development of most colon adenomas (2). Additional mutations and epigenetic changes are associated with tumor development and progression. The oncogene BMI1 is frequently overexpressed in human CRC, and the degree of upregulation correlates with disease progression and is predictive of poor patient survival (3–5). This suggests that BMI1 enables both the development and metastatic progression of CRC. Knockdown of *Bmi1* in human CRC cell lines has been shown to suppress their proliferation *in vitro* and in xenografts (6). However, the role of *Bmi1* in the initiation of autochthonous intestinal tumors has not been investigated.

Much of our understanding of Bmi1's *in vivo* role has come from analysis of germline $Bmi1^{-/-}$ mice (7). These animals have a shortened lifespan and they display cerebellar and hematopoietic abnormalities. These tissue defects reflect a requirement for *Bmi1* to maintain the self-renewal and proliferative capacity of adult neuronal and hematopoietic stem/progenitor cells via epigenetic silencing of the *Ink4a-Arf* and *Cdkn1a* loci (8–10). Bmi1's ability to silence these tumor suppressors and promote stem cell characteristics has been linked to Bmi1's oncogenic activity in various tumor types (9, 11). In CRC, intestinal stem cells are thought to be the targets of transformation (12), reflecting the importance of Wnt/β-catenin signaling in the maintenance of these cells. *Bmi1* is expressed in intestinal stem cell populations, including both the +4 position and $LGR5^{+}$ cells (13–15), but its requirement for their function has not been demonstrated. Here, we use mouse models to assess the requirement for *Bmi1* in the development of autochthonous small intestinal tumors and show that it plays a crucial role.

Results and Discussion

To investigate Bmi1's role in intestinal tumorigenesis, we took advantage of an established mouse model in which a single conditional Apc^{fl} allele (16) is inactivated throughout the intestinal epithelium using the *Vil-cre* transgene (17). After somatic recombination of the wildtype *Apc* allele, these mice develop numerous small intestinal adenomas and a lower incidence of colon adenomas (18). The resulting tumor load causes morbidity between 100–140 days of age. Importantly, this precedes the typical maximal lifespan of germline $Bmi1^{-/-}$ adult mice (approximately 150 days), allowing us to intercross these mice and assess how germline *Bmi1* mutation affects the tumor phenotype of *Apc;Vil-cre* mice. We generated cohorts of $Apc^{fl/+}$*;Vil-cre* mice that were $Bmi1^{+/+}$, $Bmi1^{+/-}$ or $Bmi1^{-/-}$. Males and females were considered separately because intestinal tumorigenesis is gender dependent (18). Any graph showing pooled data from male and female mice (as noted in the figure legend), illustrates a phenotype that is overtly present in both sexes. Initially, we examined the tumor phenotypes of 120 day old mice. We found that visible small intestinal tumors were numerous in $Bmi1^{+/+}$ animals, but almost completely absent in $Bmi1^{-/-}$ mice (Figure 1a,b). *Bmi1* heterozygotes displayed an intermediate phenotype, suggesting a dose-dependent effect (Figure 1b). Analysis of all tumors (visible by eye or microscopic analysis)

NIH-PA Author Manuscript

NIH-PA Author Manuscript

NIH-PA Author Manuscript

confirmed that *Bmi1* mutation caused a significant, dose-dependent reduction in the size of small adenomas (Figure 1c). Indeed, the median and maximal cross-sectional areas (CSA) of *Bmi1*$^{-/-}$ adenomas were more than tenfold lower than those of *Bmi1*$^{+/+}$ tumors (Figure 1c). Additionally, even when considering lesions of any size, *Bmi1*$^{-/-}$ mice had significantly fewer small intestinal adenomas ($p<0.001$) than *Bmi1*$^{+/+}$ controls (Figure 1d). Importantly, *Bmi1* status did not alter the efficiency of Cre-mediated recombination (Supplemental Figure 1a) or impair key oncogenic events arising from *Apc* inactivation including accumulation of nuclear β-Catenin and c-Myc (Supplemental Figure 1b). Thus, we conclude that *Bmi1* mutation acts in a dose-dependent manner to suppress small intestinal tumor development.

We also examined the effect of *Bmi1* mutation on colon adenomas, and found that *Bmi1*$^{-/-}$ animals had fewer visible tumors than *Bmi1*$^{+/+}$ controls (Supplemental Figure 2a,b). Unfortunately, because colon tumors arise at low frequency in *Apc*$^{fl/+}$*;Vil-cre* mice it was difficult to establish statistical significance, and this was only achieved for male mice (Supplemental Figure 2b). Given this challenge, we decided to focus on the small intestinal phenotype. First, we wanted to determine the effect of *Bmi1* mutation at earlier stages of tumor development, and thus examined 90 day animals. At this younger age, we also observed significantly fewer ($p<0.01$) and smaller ($p<0.01$) lesions in *Bmi1*$^{-/-}$ animals versus *Bmi1*$^{+/+}$ controls (Figure 1d,e). Moreover, our comparison of the 90 and 120 day time points showed that these two genotypes had differential effects on tumor progression (Figure 1d,e). In *Bmi1*$^{+/+}$ mice, tumor number did not change significantly between 90 and 120 days, but tumor size increased significantly ($p<0.05$). In contrast, *Bmi1*$^{-/-}$ mice showed no increase in median tumor size between 90 and 120 days. Furthermore, the incidence of tumors decreased significantly ($p<0.01$) between these two ages. Taken together, these findings suggest that *Bmi1* loss suppresses small intestinal tumor progression and maintenance.

We wanted to determine how *Bmi1* loss impedes tumor progression. In many other tumor types, Bmi1's oncogenic activity is at least partially dependent upon its ability to repress the *Ink4a/Arf* locus (19). Thus, we wanted to explore the potential contribution of the p16^{Ink4a} and p19^{Arf} tumor suppressors. While we could not perform western blot for p16^{Ink4a} and p19^{Arf} in *Bmi1*$^{-/-}$ adenomas because of their small size, and reliable detection by immunohistochemistry in the intestine has not been demonstrated, we were able to screen wildtype and *Bmi1*$^{+/-}$ adenomas for these proteins. These two genotypes showed no obvious difference in p16^{Ink4a} levels (Supplemental Figure 3a), but p19^{Arf} was typically elevated in *Bmi1*$^{+/-}$ tumors, compared to *Bmi1*$^{+/+}$ controls (Figure 2a). Given this, it seemed likely that p19^{Arf} was also upregulated in *Bmi1*$^{-/-}$ tumors. Thus, we examined the small intestinal adenomas for the known tumor suppressive effects of p19^{Arf}. Initially, we assayed for senescence-associated β-galactosidase (SA-βgal). However, we saw no detectable differences between *Bmi1*$^{+/+}$ versus *Bmi1*$^{-/-}$ adenomas at either 90 days (little detectable SA-βgal) or 120 days (low level SA-βgal staining; Supplemental Figure 3b). Next, we assessed the proliferative index of adenomas by quantification of BrdU incorporation at 90 days (Figure 2b). Unexpectedly, the proportion of proliferating cells was significantly higher in *Bmi1* mutant adenomas than *Bmi1*$^{+/+}$ controls, even when controlling for tumor size (Figure 2b). Thus, neither enhanced senescence nor impaired proliferation can account for

NIH-PA Author Manuscript

NIH-PA Author Manuscript

NIH-PA Author Manuscript

the tumor suppressive effects of Bmi1 loss. Finally, we assayed for apoptosis by quantification of cleaved caspase-3 in adenomas at 90 days (Figure 2c). We found that this was increased significantly ($p<0.01$) in smaller (CSA<10^4 μm^2) *Bmi1*$^{-/-}$ adenomas, but not in larger *Bmi1*$^{-/-}$tumors. We also detected cleaved caspase-3 in non-transformed regions of *Bmi1*$^{-/-}$ jejunum and ileum, including in *Bmi1*$^{-/-}$mice that lacked *Vil-cre* and therefore *Apc* inactivation (Supplemental Figure 4a–c). Thus, *Bmi1* loss increased the predisposition of emerging intestinal adenomas, and also normal intestinal epithelium, to undergo apoptosis.

p19^{Arf} is known to promote apoptosis through stabilization of p53 (20). Thus, we screened for p53 levels in adenomas by immunohistochemical staining (Figure 2d). The mean percentage of p53-positive nuclei was significantly higher in *Bmi1*$^{-/-}$ adenomas than in either *Bmi1*$^{+/+}$ or *Bmi1*$^{+/-}$ adenomas ($p<0.01$). Indeed, 64% of *Bmi1*$^{-/-}$ adenomas, but 0% of *Bmi1*$^{+/+}$ adenomas, had more than 25% p53-positive nuclei. Notably, we observed p53 stabilization in both smaller (CSA<10^4 μm^2) and larger *Bmi1*$^{-/-}$ tumors (data not shown), even though only the small lesions had elevated apoptosis. This raised the question of whether the stabilized p53 was wildtype or mutant, particularly in the larger *Bmi1*$^{-/-}$ tumors. To address this question, we used laser capture to isolate DNA from *Bmi1*$^{-/-}$ and wildtype small intestinal tumors, and screened for *p53* mutations by PCR and sequencing of exons 5–9 (Supplemental Figure 5). Unexpectedly, all of these sequences were wildtype (data not shown). Thus, we conclude that p53 is activated in a high fraction of *Bmi1*$^{-/-}$ adenoma cells but elevated apoptosis is somehow limited to the smaller tumors.

We wanted to assess the degree to which p19^{Arf} contributes to the phenotypes of *Bmi1* mutant tumors. Thus, we crossed an *Arf* null strain (21) into our mouse model to generate *Apc*$^{fl/+}$*;Vil-cre* mice that were wildtype, *Arf*$^{-/-}$, *Bmi1*$^{-/-}$ or *Bmi1*$^{-/-}$*;Arf*$^{-/-}$. Since the introduction of mutant *Arf* caused some animals to develop tumor-associated morbidity (cachexia and hunching) by 90 days, we selected this age for analysis (Figure 3). Previous studies showed that *Ink4a/Arf*$^{-/-}$ mice have a lower small intestinal tumor burden than wildtype controls (22). Consistent with this report, we found that *Arf*$^{-/-}$ mice had a similar tumor incidence as wildtype controls (Figure 3a,b) but the median size of these *Arf*$^{-/-}$ tumors was significantly reduced ($p<0.01$; Figure 3a,c). In stark contrast, *Bmi1*$^{-/-}$*;Arf*$^{-/-}$ mice had a significant increase in both the number ($p<0.01$; Figure 3a,b) and size ($p<0.001$; Figure 3a,c) of small intestinal adenomas, compared to *Bmi1*$^{-/-}$ animals. Indeed, the tumor phenotypes of these *Bmi1*$^{-/-}$*;Arf*$^{-/-}$ animals now approached that of the *Arf*$^{-/-}$ animals (Figure 3); there was no significance difference in total tumor number (Figure 3b) or tumor size (Figure 3c) between these two genotypes, but *Bmi1*$^{-/-}$*;Arf*$^{-/-}$ mice did have significantly fewer visible lesions than *Arf*$^{-/-}$ animals ($p<0.01$, data not shown) suggesting that the rescue is not complete. Because we cannot follow the cohort beyond 90 days, we were unable to determine whether *Arf* loss altered the influence of *Bmi1*-deficiency on the progression and/or maintenance of tumors between 90 to 120 days. Importantly, analysis of the 90 day tumors showed that *Arf* loss significantly suppressed the elevation of cleaved caspase 3 ($p<0.05$, Figure 2c), and the stabilization of p53 (Figure 2d; $p<0.01$), within the *Bmi1*$^{-/-}$ adenomas. Thus, we conclude that *Arf* plays a major role in the ability of *Bmi1* deficiency to suppress small intestinal tumors through activation of p53 and induction of apoptosis.

NIH-PA Author Manuscript

NIH-PA Author Manuscript

NIH-PA Author Manuscript

We had previously noted the Bmi1 deficiency also causes apoptosis within the normal intestinal epithelium (Supplemental Figure 4). Unexpectedly, our analysis of the *Bmi1*$^{-/-}$;*Arf*$^{-/-}$ compound mutant mice showed that *Arf* inactivation had no significant impact on this normal tissue apoptosis. Thus, *Bmi1* loss promotes apoptosis through distinct mechanisms in normal, versus transformed, intestinal epithelium. We wished to establish whether the *Bmi1* mutant tumor suppression was intrinsic to the intestinal epithelium. To address this, we engineered a conditional *Bmi1* (*Bmi1*^{fl}) mutant mouse strain that allowed Cre-dependent deletion of Bmi1 core functions (encoded by exons 4–8), and confirmed that this conditional *Bmi1* mutant allele recapitulates all of the developmental defects characteristic of germline *Bmi1* mutants (Supplemental Figure 6).

We used this conditional allele to generated cohorts of *Bmi1*$^{fl/fl}$;*Apc*$^{fl/+}$;*Vil-cre* mice and *Apc*$^{fl/+}$;*Vil-cre* controls, and compared their small intestinal tumor to each other, and to that of germline *Bmi1*$^{-/-}$;*Apc*$^{fl/+}$;*Vil-cre* mice. Initially, we examined animals at 120 days. We found that the intestine-specific *Bmi1* deletion significantly reduced the number of visible lesions ($p<0.0001$, Figure 4a,b), the number of total lesions ($p<0.001$, Figure 4c) and the size of lesions ($p<0.05$, Figure 4d) in the small intestine. Importantly, the conditional *Bmi1* mutant phenotypes were all indistinguishable from those yielded by germline *Bmi1* deletion (Figure 4a–d). We also examined the tumor phenotypes in 90 day old mice to address the issue of progression and maintenance. At this time point, mice the intestinal-specific deletion of *Bmi1* also resulted in significantly fewer ($p <0.05$) and smaller ($p<0.01$) lesions that the *Bmi1*$^{+/+}$ controls (data not shown). Moreover, exactly as seen in germline *Bmi1*$^{-/-}$;*Apc*$^{fl/+}$;*Vil-cre* mutants (Figure 4e,f), *Bmi1*$^{fl/fl}$;*Apc*$^{fl/+}$;*Vil-cre* mice had significantly more adenomas at 90 versus 120 days ($p<0.01$, Figure 4e), and there was no increase in tumor size between these two time points (Figure 4f). Thus, the ability of Bmi1 deficiency to suppress the progression, and maintenance, of small intestinal tumors reflects an intrinsic defect of the transformed epithelium. To complement this, we also examined the level of apoptosis and the induction of p53 within the small intestinal adenomas. As anticipated, given the observed tumor suppression, conditional *Bmi1* deletion promoted both the stabilization of p53, and elevated levels of apoptosis, in a similar manner to germline *Bmi1* loss (data not show). Finally, we screened for apoptosis in the normal epithelium. In this setting, the intestinal specific deletion of *Bmi1* gave no induction of cleaved caspase 3 (data not shown), in stark contrast to the significantly increased cleaved caspase 3 levels resulting from germline Bmi1 mutation ($p<0.01$, Supplementary Figure 4). This further distinguishes the normal epithelial apoptosis from that of the adenomas, by showing that it is both *Arf* independent and non-cell autonomous.

We initiated this study because of the known presence of high Bmi1 expression in human CRC (4, 5). Our goal was to assess the requirement for Bmi1 in the context of autochthonous intestinal tumors. Our data clearly show that Bmi1 loss reduces both the number and size of small intestinal adenomas. Additionally, as Bmi1 animals age, we actually see a reduction in the tumor burden that reflects an apparent cap on tumor size, and a clear reduction in the total number of tumors. Thus, taken together, these data support a key role for *Bmi1* in tumor development, progression and maintenance. This tumor suppression correlates with upregulation of *Arf*, stabilization of p53 and a significant

NIH-PA Author Manuscript

NIH-PA Author Manuscript

NIH-PA Author Manuscript

increase in the level of apoptosis in smaller adenomas. Our analysis of *Arf* null mice showed that these molecular changes are linked, and that they make a major contribution to anti-tumorigenic effect of Bmi1 loss in small intestinal adenomas. Finally, our data show that the *Arf*-dependent induction of apoptosis, and the consequent tumor suppression, reflects a cell autonomous requirement for *Bmi1* within the intestinal epithelium.

Supplementary Material

Refer to Web version on PubMed Central for supplementary material.

Acknowledgments

The authors dedicate this paper to the memory of Officer Sean Collier, for his caring service to the MIT community and for his sacrifice. This work was supported by an NCI/NIH grant to J.A.L. who is a Ludwig Scholar at MIT, and fellowships to M.A.M. (CIHR), R.F. (Ludwig) and K.I.H. (NSF). We thank the Koch Institute Swanson Biotechnology Center for key technical support, particularly personnel in the ES Cell & Transgenic, Histology and Microscopy facilities. We also thank Sylvie Robine (Institut Curie) for the *Vil-cre* mouse and members of the Lees and Jacks labs for thoughtful comments.

References

1. Ferlay J, Shin HR, Bray F, Forman D, Mathers C, Parkin DM. Estimates of worldwide burden of cancer in 2008: GLOBOCAN 2008. International journal of cancer Journal international du cancer. Dec 15; 2010 127(12):2893–2917. [PubMed: 21351269]
2. Fearon ER. Molecular genetics of colorectal cancer. Annual review of pathology. 2011; 6:479–507.
3. Glinsky GV, Berezovska O, Glinskii AB. Microarray analysis identifies a death-from-cancer signature predicting therapy failure in patients with multiple types of cancer. The Journal of clinical investigation. Jun; 2005 115(6):1503–1521. [PubMed: 15931389]
4. Tateishi K, Ohta M, Kanai F, Guleng B, Tanaka Y, Asaoka Y, et al. Dysregulated expression of stem cell factor Bmi1 in precancerous lesions of the gastrointestinal tract. Clinical cancer research : an official journal of the American Association for Cancer Research. Dec 1; 2006 12(23):6960–6966. [PubMed: 17145814]
5. Li DW, Tang HM, Fan JW, Yan DW, Zhou CZ, Li SX, et al. Expression level of Bmi-1 oncoprotein is associated with progression and prognosis in colon cancer. J Cancer Res Clin Oncol. Jul; 2010 136(7):997–1006. [PubMed: 20024662]
6. Yu T, Chen X, Zhang W, Colon D, Shi J, Napier D, et al. Regulation of the potential marker for intestinal cells, Bmi1, by beta-catenin and the zinc finger protein KLF4: implications for colon cancer. The Journal of biological chemistry. Feb 3; 2012 287(6):3760–3768. [PubMed: 22170051]
7. van der Lugt NM, Domen J, Linders K, van Roon M, Robanus-Maandag E, te Riele H, et al. Posterior transformation, neurological abnormalities, and severe hematopoietic defects in mice with a targeted deletion of the bmi-1 proto-oncogene. Genes Dev. Apr 1; 1994 8(7):757–769. [PubMed: 7926765]
8. Fasano CA, Dimos JT, Ivanova NB, Lowry N, Lemischka IR, Temple S. shRNA knockdown of Bmi-1 reveals a critical role for p21-Rb pathway in NSC self-renewal during development. Cell stem cell. Jun 7; 2007 1(1):87–99. [PubMed: 18371338]
9. Gieni RS, Hendzel MJ. Polycomb group protein gene silencing, non-coding RNA, stem cells, and cancer. Biochemistry and cell biology = Biochimie et biologie cellulaire. Oct; 2009 87(5):711–746. [PubMed: 19898523]
10. Subkhankulova T, Zhang X, Leung C, Marino S. Bmi1 directly represses p21Waf1/Cip1 in Shh-induced proliferation of cerebellar granule cell progenitors. Molecular and cellular neurosciences. Oct; 2010 45(2):151–162. [PubMed: 20600931]
11. Abdouh M, Facchino S, Chatoo W, Balasingam V, Ferreira J, Bernier G. BMI1 sustains human glioblastoma multiforme stem cell renewal. The Journal of neuroscience : the official journal of the Society for Neuroscience. Jul 15; 2009 29(28):8884–8896. [PubMed: 19605626]

NIH-PA Author Manuscript

NIH-PA Author Manuscript

NIH-PA Author Manuscript

12. Barker N, Ridgway RA, van Es JH, van de Wetering M, Begthel H, van den Born M, et al. Crypt stem cells as the cells-of-origin of intestinal cancer. Nature. Jan 29; 2009 457(7229):608–611. [PubMed: 19092804]

13. Sangiorgi E, Capecchi MR. Bmi1 is expressed in vivo in intestinal stem cells. Nature genetics. Jul; 2008 40(7):915–920. [PubMed: 18536716]

14. van der Flier LG, van Gijn ME, Hatzis P, Kujala P, Haegebarth A, Stange DE, et al. Transcription factor achaete scute-like 2 controls intestinal stem cell fate. Cell. Mar 6; 2009 136(5):903–912. [PubMed: 19269367]

15. Tian H, Biehs B, Warming S, Leong KG, Rangell L, Klein OD, et al. A reserve stem cell population in small intestine renders Lgr5-positive cells dispensable. Nature. Oct 13; 2011 478(7368):255–259. [PubMed: 21927002]

16. Colnot S, Niwa-Kawakita M, Hamard G, Godard C, Le Plenier S, Houbron C, et al. Colorectal cancers in a new mouse model of familial adenomatous polyposis: influence of genetic and environmental modifiers. Lab Invest. Dec; 2004 84(12):1619–1630. [PubMed: 15502862]

17. el Marjou F, Janssen KP, Chang BH, Li M, Hindie V, Chan L, et al. Tissue-specific and inducible Cre-mediated recombination in the gut epithelium. Genesis. Jul; 2004 39(3):186–193. [PubMed: 15282745]

18. Hinoi T, Akyol A, Theisen BK, Ferguson DO, Greenson JK, Williams BO, et al. Mouse model of colonic adenoma-carcinoma progression based on somatic Apc inactivation. Cancer Res. Oct 15; 2007 67(20):9721–9730. [PubMed: 17942902]

19. Grinstein E, Wernet P. Cellular signaling in normal and cancerous stem cells. Cell Signal. Dec; 2007 19(12):2428–2433. [PubMed: 17651940]

20. Sherr CJ, Bertwistle D, DENB W, Kuo ML, Sugimoto M, Tago K, et al. p53-Dependent and -independent functions of the Arf tumor suppressor. Cold Spring Harbor symposia on quantitative biology. 2005; 70:129–137.

21. Kamijo T, Zindy F, Roussel MF, Quelle DE, Downing JR, Ashmun RA, et al. Tumor suppression at the mouse INK4a locus mediated by the alternative reading frame product p19ARF. Cell. Nov 28; 1997 91(5):649–659. [PubMed: 9393858]

22. Gibson SL, Dai CY, Lee HW, DePinho RA, Gee MS, Lee WM, et al. Inhibition of colon tumor progression and angiogenesis by the Ink4a/Arf locus. Cancer research. Feb 15; 2003 63(4):742–746. [PubMed: 12591718]

23. Soriano P. Generalized lacZ expression with the ROSA26 Cre reporter strain. Nat Genet. Jan; 1999 21(1):70–71. [PubMed: 9916792]

24. Dimri GP, Lee X, Basile G, Acosta M, Scott G, Roskelley C, et al. A biomarker that identifies senescent human cells in culture and in aging skin in vivo. Proc Natl Acad Sci U S A. Sep 26; 1995 92(20):9363–9367. [PubMed: 7568133]

25. Tallquist MD, Soriano P. Epiblast-restricted Cre expression in MORE mice: a tool to distinguish embryonic vs. extra-embryonic gene function. Genesis. Feb; 2000 26(2):113–115. [PubMed: 10686601]

NIH-PA Author Manuscript
NIH-PA Author Manuscript
NIH-PA Author Manuscript

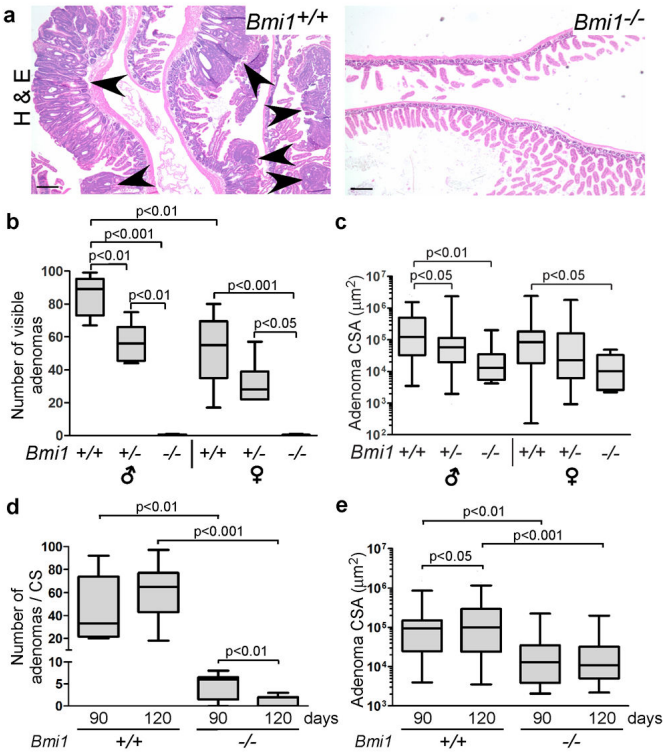

Figure 1. *Bmi1* is required for small intestinal adenoma development, progression and maintenance

a Representative Haematoxylin & Eosin stained sections of small intestine from 120 day old *Apc*$^{fl/+}$;*Vil-cre* mice show adenomas (marked by arrowheads) in *Bmi1*$^{+/+}$ but not *Bmi1*$^{-/-}$ context. Original magnification 4X. Scale bar represents 200 μm. **b,c** Quantification of **(b)** the number of visible (diameter > 1mm) adenomas, and **(c)** the cross-sectional area (CSA) of all adenomas, in 120-day old animals according to *Bmi1* status and gender (n= 4–8). **d,e** Comparison of **(d)** the total number of small intestinal adenomas per histological cross-section (CS), and **(e)** adenoma cross-sectional area (CSA), in 90-day old versus 120-day old mice shows that *Bmi1* is required for their maintenance and progression. Data were pooled for male and females, using equal numbers of each (n=8–10 for combined genders). For **(a–e)** mouse small intestine was dissected, fixed in formalin, coiled and subject to histological processing followed by paraffin embedding. Sections were examined using a Nikon Eclipse E600 microscope with a SPOT RT digital camera. SPOT Basic imaging software was utilized for capture and area/length measurements. Data are presented as box plots with marked median values and whiskers spanning the 5th to the 95th percentiles. For statistical analyses **(b,c)** ANOVA was performed with a Tukey post-test for paired comparisons or **(d,e)** a student's 2-sided t-test was performed for paired comparisons.

NIH-PA Author Manuscript

NIH-PA Author Manuscript

NIH-PA Author Manuscript

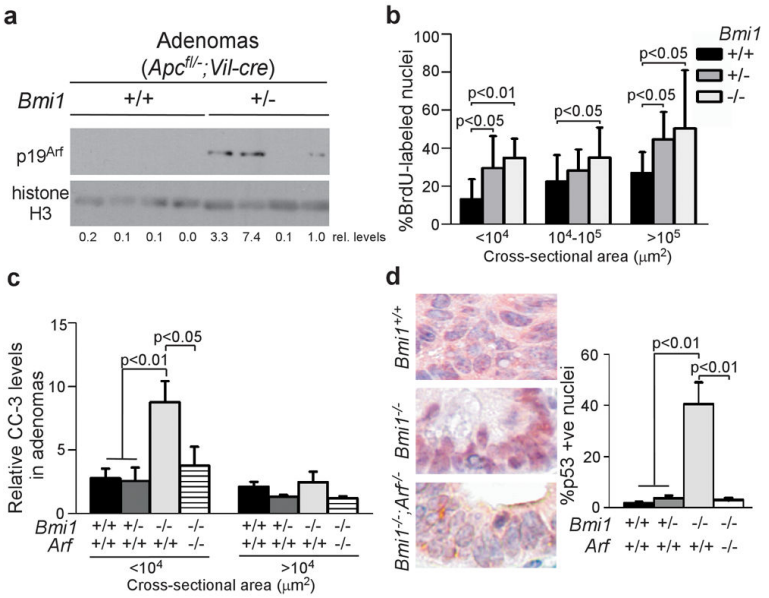

Figure 2. *Bmi1* loss promotes *Arf*-dependent, p53 stabilization and apoptosis within small intestinal adenomas

a Western blot of lysates from small intestinal adenomas demonstrates higher $p19^{Arf}$ expression in $Bmi1^{+/-}$ versus $Bmi1^{+/+}$ adenomas. Lysates were prepared from small intestinal adenomas that were minced, digested for 1 hour at 37°C in dispase (150 u/ml final; Gibco, Japan), triturated and lysed in RIPA buffer (200 mM Tris pH 7.4, 130 mM NaCl, 10% glycerol, 0.1% SDS, 0.5% DOC, 1% Triton) containing protease inhibitors (Roche, Germany). Protein was separated by SDS-PAGE and western blot was performed with anti-$p19^{Arf}$ (top panel; BD Biosciences, San Jose CA, NB200-106) and Histone H3 (lower panel; Cell Signaling, Danvers MA, 4620) antibodies, followed by incubation with a 1:5000 dilution of HRP-conjugated secondary antibodies (Cell Signaling, Danvers, MA). Relative levels of $p19^{Arf}$ were quantified and normalized to levels of Histone H3 after band density measurements using ImageJ software. **b** $Bmi1^{+/-}$ and $Bmi1^{-/-}$ adenomas are more proliferative than $Bmi1^{+/+}$ adenomas in 90-day old mice, as determined by quantification of the average percentage of adenoma nuclei staining positive for incorporated BrdU. Data were stratified by adenoma cross-sectional area. BrdU (10 μg/g body weight; Sigma, St. Louis MO) was injected I.P. two hours prior to euthanasia. **c** Analysis of average number of cleaved caspase-3 positive adenoma cells, normalized to adenoma cross-sectional area, shows that *Bmi1* deficiency elevated apoptosis in the smallest adenomas in an *Arf*-dependent manner. **d** Adenomas of 90 day old $Bmi1^{-/-}$mice have an average high percentage of cells with p53 stabilization, which is lost in the absence of *Arf*. Original magnification was 40X. For **b–d**: Adenomas from at least 5 mice of each genotype consisting of both males and females were assayed. Immunohistochemistry on intestinal sections was performed after antigen retrieval in 10 mM citric acid pH 6.0 using a decloaking chamber, followed by standard DAB protocol and haematoxylin counterstain. Antibodies were: anti-BrdU (1:100; Beckton Dickson, Franklin Lakes NJ, 347580), p53 (1:500, Santa Cruz, Santa Cruz CA, FL-393) and cleaved caspase-3 (1:1000, Cell Signaling, Danvers MA, 9661). Tissue

processing, image capture/measurements and statistical analysis were performed as described for Figure 1b,c and error bars represent standard deviation.

NIH-PA Author Manuscript
NIH-PA Author Manuscript
NIH-PA Author Manuscript

NIH-PA Author Manuscript
NIH-PA Author Manuscript
NIH-PA Author Manuscript

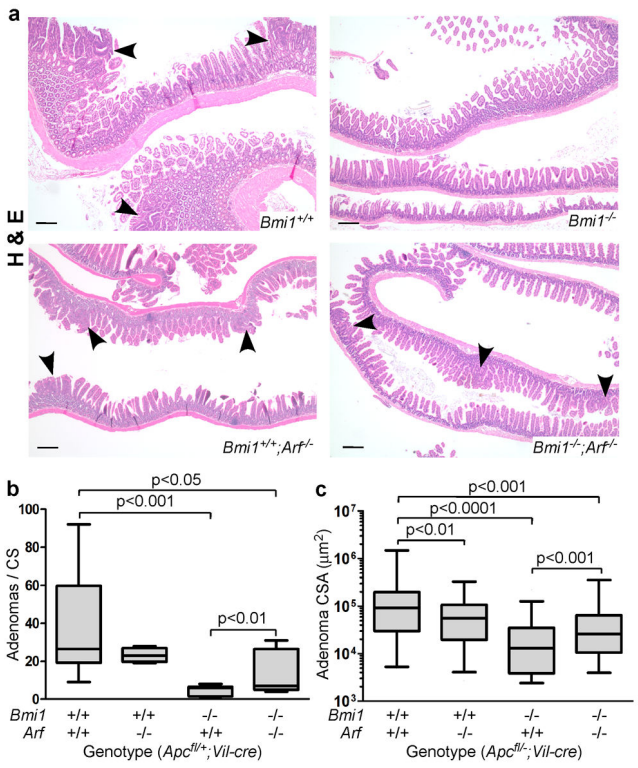

Figure 3. The tumor suppressive effects of *Bmi1* deficiency are *Arf*-dependent

a Representative Haematoxylin & Eosin stained sections of small intestine from 90 day old $Apc^{fl/+}$;*Vil-cre* mice show adenomas (marked by arrowheads) in a $Bmi1^{+/+}$, $Bmi1^{+/+}$;$Arf^{-/-}$, $Bmi1^{-/-}$;$Arf^{-/-}$ but not $Bmi1^{-/-}$ context. Original magnification 4X. Scale bar represents 200 μm. **b,c** Quantification of the effect of *Bmi1* and *Arf* status on (**b**) the total number of adenomas per cross-section (CS) and (**c**) adenoma size, as measured by cross-sectional area (CSA), in 90 day old $Apc^{fl/+}$;*Vil-cre* mice (n≥5 for each genotype consisting of both males and females) shows that *Arf* loss suppresses $Bmi1^{+/+}$ tumors while promoting $Bmi1^{-/-}$ tumors. Tissue processing and image capture/measurements were performed as described for Figure 1. For statistical analysis, ANOVA was performed, followed by an Unpaired Fisher's LSD test for paired comparisons.

NIH-PA Author Manuscript
NIH-PA Author Manuscript
NIH-PA Author Manuscript

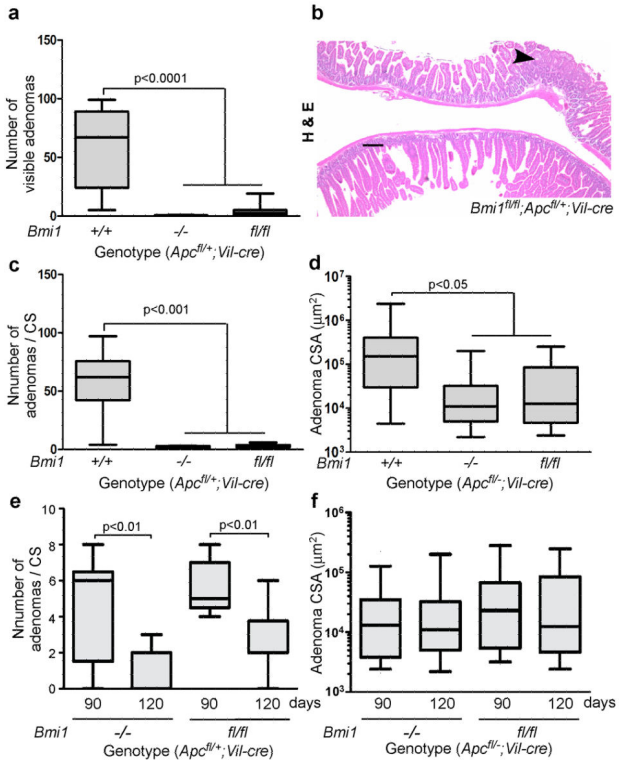

Figure 4. The oncogenic effect of *Bmi1* in small intestinal tumorigenesis reflects its action within the intestinal epithelium

a–d Comparison of **(a)** the number of visible adenomas (diameter>1 mm), **(b,c)** the total number of adenomas per cross-section (CS) and **(d)** adenoma size, as measured by CSA, shows a similar degree of tumor suppression in the small intestines of 120 day $Apc^{fl/+}$;*Vil-cre* mice that are $Bmi1^{fl/fl}$ versus $Bmi1^{-/-}$ (both genders; n=8 or greater). For **(b)**, original magnification was 4X and the scale bar represents 200 µm. **e,f** The relative **(e)** number and **(f)** size of small intestinal adenomas in $Bmi1^{-/-}$ or $Bmi1^{fl/fl}$ $Apc^{fl/+}$;*Vil-cre* mice at 90 days versus 120 days (both genders; n=5–10) phenocopies those of $Bmi1^{-/-}$;$Apc^{fl/+}$;*Vil-cre* mice. The *Bmi1* conditional allele ($Bmi1^{fl}$) was generated using standard gene targeting to insert *loxP* sites in introns 3 and 8 and validated as shown in Supplemental Figure 6. Tissue processing, image capture/measurements and statistical analyses were performed as described for Figure 1.